JOURNAL OF SOLID STATE CHEMISTRY 37, 6–15 (1981)

# Crystal Chemistry of the $(Ta_6Si_4O_{26})^{6-}$ and $(Ta_{14}Si_4O_{47})^{8-}$ Frameworks

D. P. BIRKETT, P. J. WISEMAN, AND J. B. GOODENOUGH

*Inorganic Chemistry Laboratory, South Parks Road, Oxford OX1 3QR, England*

Received August 21, 1979; in revised form April 7, 1980

The range of chemical flexibilities of the hexagonal frameworks $(Ta_6Si_4O_{26})^{6-}$ and $(Ta_{14}Si_4O_{47})^{8-}$ have been partially explored. This has been done with high-temperature preparations as in general ionic mobilities in these frameworks are too low to permit low-temperature ion exchange. Ionic site potential calculations indicate that preferential site-occupancy factors as well as geometric constraints are responsible for the absence of ionic motion. New phases $K_{6-x}Na_xTa_6Si_4O_{26}$ ($x \lesssim 4$), $K_{8-x}Na_xTa_{14}Si_4O_{47}$ ($x \lesssim 5$), and impure $Ba_{3-x}Na_{2x}Ta_6Si_4O_{26}$ have been prepared. Introduction of up to 2 moles of $Li^+$ and 1 mole of $Mg^{2+}$ ions per formula unit into sites of the framework not normally occupied has been demonstrated as well as the possibility of partially substituting $Zr^{4+}$ for $Ta^{5+}$ ions. Substitutions designed to introduce large tunnel vacancies in the presence of only monovalent $K^+$ or $Na^+$ ions (P for Si, W for Ta and F for O) generally proved unsuccessful. Competitive phases also frustrated attempts to substitute either the larger $Rb^+$ or the smaller $Li^+$ ions into the large-tunnel sites. A large area of solid solution was discovered in the $BaO–Na_2O–Ta_2O_5$ phase diagram; it has a $(TaO_3)^-$ framework with the structure of tetragonal potassium tungsten bronze.

## Introduction

An $(M_6Si_4O_{26})^{6-}$ framework having $M$ = Nb or Ta was first discovered by Shannon and Katz (*1, 2*) in the compounds $Ba_3M_6Si_4O_{26}$. Choisnet *et al.* (*3*) synthesized the same framework in the phases $Sr_3M_6Si_4O_{26}$ and $K_6M_6Si_4O_{26}$. We initiated a study of this framework in the hope of discovering a new $Na^+$ ion electrolyte.

The framework consists of infinite chains of vertex-linked $M$ octahedra grouped into triples by each $M$ octahedron of one chain sharing equatorial vertices with octahedra of two other chains; these triple chains are interconnected by sharing the remaining two vertices per octahedron with linear $Si_2O_7$ bridging units. The bridging units are pairs of vertex-linked tetrahedra. As illustrated in Fig. 1, these interconnections produce a hexagonal framework (space group $P\bar{6}2m$) having two types of tunnels running parallel to the $c$ axis: large tunnels of alternating $3(g)$ and $3(f)$ sites having pentagonal common faces perpendicular to the $c$ axis and small tunnels within the triple chains containing alternating tricapped trigonal prismatic sites $1(a)$ and $1(b)$ sharing triangular faces perpendicular to the $c$ axis. The $3(g)$ sites have (10 + 3) anion coordination, the $3(f)$ sites have (10 + 5) anion coordination, the $1(a)$ and $1(b)$ sites have (6 + 3) coordination. Within a basal plane, the $3(g)$ sites communicate with $3(g)$ sites in four neighboring large tunnels via a trigonal prismatic $2(c)$ site that is capped top and bottom by tetrahedral faces of $Si_2O_7$ units.

In the original $Ba_3M_6Si_4O_{26}$ ($M$ = Nb, Ta) compounds, the $Ba^{2+}$ ions only occupy the $3(g)$ sites. The $Sr^{2+}$ ion analogs are

0022-4596/81/040006-10$02.00/0

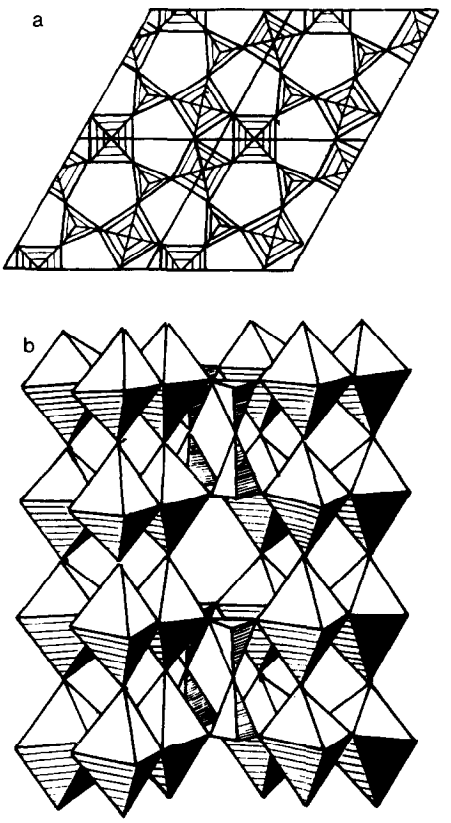


FIG. 1. The $(Ta_6Si_4O_{26})^{6-}$ framework: (a) projected onto the basal plane, and (b) viewed along a basal-plane axis.

isostructural. In the $K_6M_6Si_4O_{26}$ ($M$ = Nb, Ta) compounds, the $K^+$ ions fill both the 3($g$) and the 3($f$) sites of the large tunnels.

Evans and Katz (*4*) discovered a related structure for the reduced compound $Ba_{6+x}Nb_{14}Si_4O_{47}$. The fully oxidized compounds $K_8M_{14}Si_4O_{47}$ ($M$ = Nb, Ta) have the same $(M_{14}Si_4O_{47})$ framework (*5, 6*). This structure, which is shown in Fig. 2, is derived from the parent $Ba_3Nb_6Si_4O_{26}$ structure as follows. Every fourth layer along the $c$ axis is rotated, in its entirety, by 60° and vertically sheared into the layer below (see Fig. 2a). This results in an edge-shared cluster along the infinite chains and the replacement of the $Si_2O_7$ vertex-linked units by a single $MO_6$ octahedron. It is not surprising, therefore, to find that other repeat distances are possible; they result in compositional formulas corresponding to an intergrowth of $(M_6Si_4O_{26})$ layers alternating with $(M_8O_{21})$ layers (*6*). The pathways parallel and perpendicular to the $c$ axis are preserved, but perturbed. The structure (space group $P6_3/mcm$ $Z$ = 2) contains nine large-tunnel sites per formula unit; three (10 + 5) sites, 6($g$), and six (10 + 3) sites 12($k$). The 12($k$) sites are connected

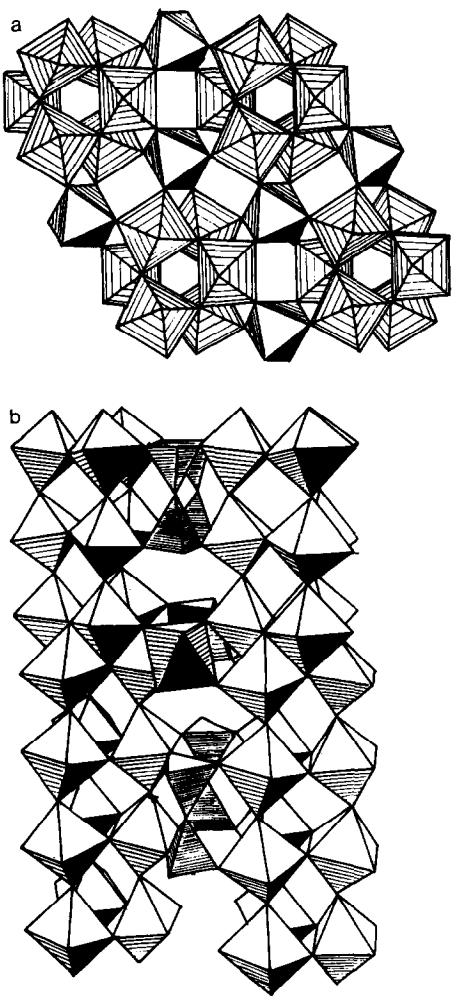


FIG. 2. The $(Ta_{14}Si_4O_{47})^{8-}$ framework: (a) projected onto the basal plane and (b) viewed along a basal-plane axis.

between tunnels by sites capped, in this case, by the tetrahedral site face of an $Si_2O_7$ unit on one side and the octahedral site face of a bridging octahedron on the other. In $Ba_{6+x}Nb_{14}Si_4O_{47}$, all the 12($k$) sites are occupied; the 6($g$) sites have only a small fractional occupancy (ca. 0.152). In $K_8Ta_{14}Si_4O_{47}$ the $K^+$ ion distribution is not known.

For $K_6Ta_6Si_4O_{26}$, the pentagonal bottleneck along the $c$ axis has center-to-anion distances of 2 × 2.59, 2 × 2.27, 1 × 1.84 Å. The largest window radius is computed as 2.1 Å, which is significantly below the sum of the $Na^+$ and $O^{2-}$ ionic radii (~2.4 Å); the hexagonal bottlenecks in the basal plane have center-to-anion distances of 4 × 2.61 and 2 × 3.17 Å, corresponding to a maximum window radius of 2.61 Å. Although these distances would alter in possible sodium derivatives, they suggest that this framework may support fast ion motion in the basal plane for ions of size not greater than sodium. Mobility will only be observed, of course, if vacancies can be introduced into the 3($g$) positions. Bottleneck sizes for $K_8Ta_{14}Si_4O_{47}$ lead to the same conclusions for this structure.

## Preparation and Characterization

Samples were generally synthesized by standard high-temperature techniques. Appropriate proportions of alkali–metal carbonates, transition-metal oxide, and silica were ground together in an agate mortar; fired at 1250°C in an alumina crucible for 18 hr; and then reground, pressed into pellets, and fired at 1400°C for a further 18 hr.

All X-ray work described in this paper was performed on powders. Preliminary powder X-ray studies were made on a Phillips PW 1050 X-ray diffractometer with a quartz analyzing monochromator, while for accurate lattice parameters a Stöe Guinier camera, with curved graphite monochromator, was employed (Cu$K\alpha$ radiation). Phases were identified by comparison of X-ray powder diffraction data with powder patterns of these phases in the literature.

Direct synthesis of the $Na_6M_6Si_4O_{26}$ ($M$ = Nb, Ta) analogs was frustrated by the formation of competitive phases, notably the perovskites $NaTaO_3$ $NaNbO_3$. With direct synthesis unsuccessful, we investigated three alternate methods of incorporating $Na^+$ ions into the basic framework:

Direct synthesis of compounds having a partial replacement of $K^+$ or $Ba^{2+}$ ions by $Na^+$ ions.

Exchange of $Na^+$ ions for $K^+$ ions by reacting the potassium analog with excess molten $NaNO_3$.

Substitution or interstitial insertions into the framework so as to make the potassium analog cation deficient before attempting $Na^+$ ion substitutions for potassium by ion exchange.

### A. $K_{6-x}Na_xTa_6Si_4O_{26}$

Substitution of $Na^+$ for $K^+$ ions in $K_6Ta_6Si_4O_{26}$ by ion exchange in molten $NaNO_3$ proved unsuccessful. Thinking this to be due to a filled set of 3($g$) and 3($f$) sites, we decided to determine the limit of sodium incorporation into the $(M_6Si_4O_{26})^{6-}$ framework by direct synthesis. Mixtures corresponding to $x$ = 1, 2, 3, 4, 4.5, and 5 were treated as described above. Powder X-ray patterns showed single hexagonal phases for $x \lesssim 3$. Table I gives the variation of lattice parameters with $x$, and Table II gives a typical powder pattern, that for $x$ = 1.

The composition $x$ = 4 was also hexagonal, but it could not be obtained free from $NaTaO_3$ even after repeated firings. From the lattice parameters of the hexagonal phase and the variation of these parameters with $x$ in the system, the solid solutions appear to extend nearly to $x$ = 4. For $x > 4$, the product consisted of mixed phases with $NaTaO_3$ predominating.

TABLE I

CRYSTALLOGRAPHIC DATA FOR THE COMPOSITIONS $K_{6-x}Na_xTa_6Si_4O_{26}$[a]

| $x$ | $a_0$ (Å) | $c_0$ (Å) | $V$ (Å$^3$) | |
|---|---|---|---|---|
| 0 | 9.066 | 7.873 | 560.4 | (3) |
| 1 | 9.045(1) | 7.843(1) | 555.7 | |
| 2 | 9.025(1) | 7.808(2) | 550.8 | |
| 2.5 | 9.011(1) | 7.807(2) | 549.0 | |
| 3 | 8.996(1) | 7.789(1) | 545.9 | |
| 4[b] | 8.973(1) | 7.769(1) | 541.7 | |

[a] All phases are hexagonal. Standard deviations in parentheses.

[b] Nominal composition.

The intractable nature of these phases precluded classical chemical analysis. A phase of nominal composition $K_{3.5}Na_{2.5}Ta_6Si_4O_{26}$ was analyzed by means of its characteristic X-ray emission spectrum using a Link Systems Ltd. X-ray analyzer on a JEOL Temscan 100 CX electron microscope with the sample supported on a nylon grid. Samples of $K_6Ta_6Si_4O_{26}$ and $NaTaO_3$ were used as calibrants. The spectra were reproducible, and molar elemental ratios of K:Ta of 0.52:1 (calc 0.58:1) and Ta:Si of 1.48:1 (calc 1.50:1) were determined. Although the presence of sodium was shown in all the crystallites examined, it could not be accurately determined due to peak overlap. We were also able to prepare these phases from well-characterized samples of $K_6Ta_6Si_4O_{26}$, $NaTaO_3$, and $SiO_2$. In this case there was no significant weight change during chemical reaction, which supports the essential correctness of the compositions reported in this work.

Since all the large-tunnel sites are filled in these compositions, ionic mobility was not anticipated and no conductivity measurements were made.

*B. $Ba_{3-x}Na_{2x}Ta_6Si_4O_{26}$*

In an initial attempt to introduce $Na^+$ ions together with large-tunnel vacancies, we investigated the system $Ba_{3-x}Na_{2x}Ta_6Si_4O_{26}$. Phases of this system would have $(3 - x)$ vacancies per formula unit in the large-tunnel sites. Powder X-ray diffraction of the products for $x \leq \frac{3}{2}$ showed two-phase mixtures consisting of a hexagonal phase with lattice parameters close to those of $Ba_3Ta_6Si_4O_{26}$ (Table III) and a tetragonal phase having lattice parameters suggestive of the tetragonal potassium tungsten bronze (TKWB) structure (Fig. 3),

TABLE II

POWDER X-RAY DATA FOR THE PHASE $K_5NaTa_6Si_4O_{26}$[a]

| Intensity | *hkl* | $d_{obs}$ (Å) | $d_{calc}$ (Å) |
|---|---|---|---|
| ms | 001 | 7.85 | 7.84 |
| s | 110 | 4.529 | 4.523 |
| s | 200 | 3.920 | 3.917 |
| ms | 201 | 3.509 | 3.504 |
| vs | 210 | 2.960 | 2.961 |
| ms | 211 | 2.770 | 2.770 |
| mw | 300 | 2.609 | 2.611 |
| s | 212 | 2.364 | 2.363 |
| mw | 220 | 2.262 | 2.261 |
| vw | 203 | 2.176 | 2.174 |
| s | 213 | 1.960 | 1.960 |
| w | 401 | 1.900 | 1.900 |
| s | 320 | 1.798 | 1.797 |
| s | 321 | 1.752 | 1.752 |
| m | 223 | 1.709 | 1.710 |
| vs | 322 | 1.634 | 1.634 |
| ms | 412 | 1.567 | 1.567 |
| m | 330 | 1.508 | 1.508 |
| mw | 323 | 1.481 | 1.481 |
| w | 205 | 1.456 | 1.456 |
| s | 404 | 1.385 | 1.386 |
| s | 512 | 1.324 | 1.324 |
| m | 601 | 1.288 | 1.288 |
| m | 116 | 1.255 | 1.256 |
| w | 504 | 1.2238 | 1.2239 |
| s | 334 | 1.1950 | 1.1951 |
| w | 325 | 1.1819 | 1.1817 |
| s | 514 | 1.1430 | 1.1431 |
| w | 523 | 1.1309 | 1.1309 |
| w | 007 | 1.1207 | 1.1204 |

[a] Hexagonal lattice $a_0 = 9.054(1)$; $c_0 = 7.843(1)$.

TABLE III

CRYSTALLOGRAPHIC DATA FOR THE NOMINAL COMPOSITIONS $Ba_{3-x}Na_{2x}Ta_6Si_4O_{26}$

| | Hexagonal phases | | | | Tetragonal phases | | |
|---|---|---|---|---|---|---|---|
| $x$ | $a_0$ (Å) | $c_0$ (Å) | $V$ (Å$^3$) | | $a_0$ (Å) | $c_0$ (Å) | $V$ (Å$^3$) |
| 0.0 | 9.001 | 7.734 | 542.6 | (3) | 12.556 | 3.9465 | 622.2 |
| 0.5 | 9.067(1) | 7.601(5) | 541.2 | | 12.512(2) | 3.9222(5) | 614.0 |
| 1.0 | 8.985(2) | 7.599(3) | 531.3 | | 12.485(3) | 3.9180(5) | 610.7 |
| 1.5 | 8.983(2) | 7.570(3) | 529.0 | | 12.476(3) | 3.9099(5) | 608.6 |
| 2.0 | 8.977(2) | 7.447(3) | 519.7 | | — | — | — |

which is found for $BaTa_2O_6$. Although repeated firings increased the yield of the hexagonal phase, the tetragonal phase could not be entirely removed.

In order to positively identify the tetragonal phase, which we suspected would correspond to the formula $Ba_{1-y}Na_{2y}Ta_2O_6$, we prepared compositions with $y = 0.1$, 0.15, and 0.2. In each case we obtained a single phase having lattice parameters characteristic of a TKWB framework; see Table IV. The composition $Ba_{0.8}Na_{0.4}Ta_2O_6$, corresponding to $y = 0.2$, has complete filling of both the pentagonal and square tunnels of the TKWB framework; attempts to increase $y$ beyond 0.2 gave a two-phase mixture: $Ba_{0.8}Na_{0.4}Ta_2O_6$ and the perovskite $NaTaO_3$.

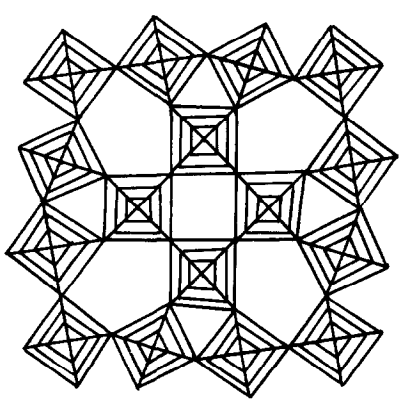

FIG. 3. The TKWB ($TaO_3^-$) framework of $BaTa_2O_6$.

Comparison of the tetragonal-phase lattice parameters of Table III with those in Table IV shows that only for the case $x = 0.5$ do the lattice parameters of the second-phase product of nominal composition $Ba_{3-x}Na_{2x}Ta_6Si_4O_{26}$ fall within the range of Table IV; the others are significantly smaller. However, the tantalate $Na_2Ta_8O_{21}$ has also been shown (7) to have a TKWB framework, but with a superstructure that triples the $b$ axis in the basal plane: $a = 12.43$ Å, $b = 3a$, $c = 3.90$ Å. Since these parameters are smaller than those of Table III, it seemed logical that the tetragonal second phases of Table III might represent solid solutions between $Na_2Ta_8O_{21}$ and $Ba_{1-y}Na_{2y}Ta_2O_6$ ($0 \leq y \leq 0.2$).

Density measurements indicate that the unit cell of $Na_2Ta_8O_{21}$ contains 4.5 formula units ($Na_9Ta_{36}O_{94.5}$). This is compatible with filling the square tunnels of the TKWB

TABLE IV

CRYSTALLOGRAPHIC DATA FOR THE COMPOSITIONS $Ba_{1-y}Na_{2y}Ta_2O_6$[a]

| $y$ | $a_0$ (Å) | $c_0$ (Å) |
|---|---|---|
| 0 | 12.556 | 3.9456 |
| 0.10 | 12.526(1) | 3.9270(5) |
| 0.15 | 12.516(1) | 3.9210(5) |
| 0.20 | 12.506(1) | 3.9160(5) |

[a] All phases are tetragonal.

framework with six $Na^+$ ions and the pentagonal tunnels containing the remaining $Na^+$ ions together with $Ta_4O_3$ groups, rather than infinite $(TaO)^{3+}$ chains, to give an overall structural formula $Na_6[Na_3(Ta_4O_3)_{3/2}]Ta_{30}O_{90}$. This awaits confirmation by a single-crystal X-ray study.

In order to determine whether solid solutions exist between the phases with a common TKWB framework ($TaO_3^-$), we prepared two intermediate compositions

$$Ba_4Na_4Ta_{18}O_{51} = 5Ba_{0.8}Na_{0.4}Ta_2O_6 \cdot Na_2Ta_8O_{21},$$
$$Ba_2Na_2Ta_{12}O_{33} = 2BaTa_2O_6 \cdot Na_2Ta_8O_{21}.$$

Both preparations gave a single-phase product with $a = 12.478(2)$, $c = 3.904(1)$ for $Ba_4Na_4Ta_{18}O_{51}$ and $a = 12.475(2)$, $c = 3.904(1)$ for $Ba_2Na_2Ta_{12}O_{33}$; very weak superstructure lines indicative of trebling of the $b$ axis, as found in $Na_2Ta_8O_{21}$, were observed for the second composition.

These results indicate the existence of a large solid-solution area in the $BaO–Na_2O–Ta_2O_5$ phase diagram. Compounds in this region crystallize with a $(TaO_3)^-$ TKWB framework; within this framework a complex cation $(Ta_xO_y)^{(5x-2y)+}$ may share the pentagonal tunnels with $Ba^{2+}$ and/or $Na^+$ ions. We have not made any experiments to determine the nature of this cation, which need not be the same as the proposed cation for $Na_2Ta_8O_{21}$. The solid-solution area probably contains the triangle formed by the system $Ba_{1-y}Na_{2y}Ta_2O_6$ ($0 \le y \le 0.2$) and $Na_2Ta_8O_{21}$ (Fig. 4).

For $x = 2$, corresponding to $BaNa_4Ta_6Si_4O_{26}$, the hexagonal phase was dominant and the major impurity was $NaTaO_3$. Since the nominal phase has only five-sixths of the large-tunnel sites occupied, we selected a sample having the largest percentage of hexagonal phase for dielectric studies. Gold electrodes were evaporated onto the two polished surfaces of a dense ceramic disk. The complex admittance was obtained with a Hewlett–Packard 1400A vector impedance meter using a frequency range of 5–500 kHz; the temperature range was 0–860°C. There was no evidence of ionic mobility, even at the highest temperatures. The conductivity at 300°C was estimated to be $3 \times 10^{-8}$ $(\Omega\text{-cm})^{-1}$.

### C. $K_{8-x}Na_xTa_{14}Si_{14}O_{47}$

Only eight-ninths of the large-channel sites are occupied in $K_8Ta_{14}Si_4O_{47}$. Nevertheless, replacement of $K^+$ by $Na^+$ ions in an excess of molten $NaNO_3$ proved unsuccessful, which is a clear indication that the $K^+$ ions are not mobile in this phase.

In order to determine whether this lack of ionic mobility applies to the $Na^+$ ions as well, we attempted to prepare the compositions $K_{8-x}Na_xTa_{14}Si_4O_{47}$. For $x = 2$ and 4, single phases resulted; the lattice parameters and cell volumes were slightly smaller than those of $K_8Ta_{14}Si_4O_{47}$; see Tables V and VI. Attempts to prepare $K_3Na_5Ta_{14}Si_4O_{47}$ gave similar results, but with a small amount of $Na_2Ta_4O_{11}$ as an

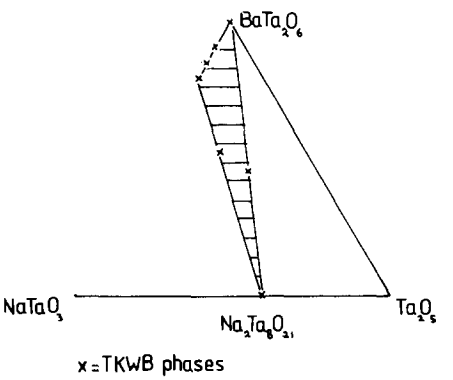


FIG. 4. Compositions $x$ shown to have the $(TaO_3)^-$ framework of the TKWB structure.

TABLE V

CRYSTALLOGRAPHIC DATA FOR PHASES RELATED TO $K_8Ta_{14}Si_4O_{47}$[a]

| Phase | $a_0$ (Å) | $c_0$ (Å) | $V$ (Å$^3$) | |
|---|---|---|---|---|
| Indexed phase from nominal composition $K_9Ta_{13}ZrSi_4O_{47}$ | 9.074(3) | 27.97(6) | 1994.4 | |
| $K_8Ta_{14}Si_4O_{47}$ | 9.046 | 27.91 | 1977.9 | (5) |
| $K_6Na_2Ta_{14}Si_4O_{47}$ | 9.027(1) | 27.843(6) | 1964.7 | |
| $K_4Na_4Ta_{14}Si_4O_{47}$ | 9.018(1) | 27.764(5) | 1955.3 | |
| $K_3Na_5Ta_{14}Si_4O_{47}$[b] | 9.009(2) | 27.76(1) | 1951.2 | |

[a] All phases are hexagonal.
[b] Nominal composition.

impurity that remained after repeated firings. The purest sample of this material was prepared as a ceramic disk of density in excess of 85% of the theoretical value. Gold electrodes were evaporated onto the two polished surfaces, and the complex admittance was measured from 5 Hz to 500 kHz and from 0 to 510°C. There was no evidence of ionic mobility, even at the highest temperatures. We obtained a conductivity at 300°C of only $7 \times 10^{-8}$ $(\Omega\text{-cm})^{-1}$.

We also attempted the preparation of $K_9ZrTa_{13}Si_4O_{47}$ at 1350°C. $K_2Ta_4O_{11}$ appeared as a second-phase impurity along with a dominant hexagonal phase having a pattern similar to $K_8Ta_{14}Si_4O_{47}$, but with a somewhat larger cell volume. This indicates that the occupancy of the tunnel sites can be varied, but we did not pursue the matter further.

### *D. Framework Substitutions*

An alternate method of varying the tunnel-site occupancy is to substitute for silicon or oxygen in the framework. In an attempt to reduce the $K^+$ occupancy of $K_6Ta_6Si_4O_{26}$, we elected to investigate the possibility of stabilizing $K_{6-x}Ta_6Si_{4-x}P_xO_{26}$ and $K_{6-x}Ta_6Si_4O_{26-x}F_x$ using $NH_4H_2PO_4$ and KF as sources of phosphorus and fluorine. In every case we obtained a mixed phase in which $K_6Ta_6Si_4O_{26}$ and

TABLE VI

POWDER X-RAY DATA FOR THE PHASE $K_6Na_2Ta_{14}Si_4O_{47}$[a]

| Intensity | *hkl* | $d_{obs}$ (Å) | $d_{calc}$ (Å |
|---|---|---|---|
| m | 002 | 14.02 | 13.92 |
| s | 100 | 7.85 | 7.82 |
| mw | 004 | 6.97 | 6.96 |
| m | 006 | 4.643 | 4.640 |
| s | 111 | 4.458 | 4.455 |
| vw | 113 | 4.059 | 4.059 |
| s | 200 | 3.913 | 3.909 |
| w | 114 | 3.789 | 3.787 |
| vw | 115 | 3.509 | 3.506 |
| m | 008 | 3.479 | 3.480 |
| mw | 204 | 3.407 | 3.408 |
| w | 116 | 3.239 | 3.235 |
| ms | 108 | 3.179 | 3.179 |
| vs | 117 | 2.986 | 2.984 |
| vs | 210 | 2.955 | 2.955 |
| vs | 211 | 2.938 | 2.938 |
| w | 213 | 2.814 | 2.815 |
| vw | 0010 | 2.782 | 2.784 |
| w | 118 | 2.757 | 2.756 |
| vw | 214 | 2.720 | 2.720 |
| m | 300 | 2.605 | 2.606 |
| m | 208 | 2.597 | 2.599 |
| w | 216 | 2.494 | 2.492 |
| w | 304 | 2.440 | 2.440 |
| s | 217 | 2.371 | 2.372 |
| vw | 306 | 2.273 | 2.272 |
| mw | 218 | 2.251 | 2.252 |
| vw | 1112 | 2.064 | 2.064 |
| m | 0014 | 1.989 | 1.989 |
| s | 400 | 1.954 | 1.954 |
| w | 1014 | 1.929 | 1.927 |
| ms | 228 | 1.893 | 1.893 |
| m | 318 | 1.840 | 1.840 |
| vw | 406 | 1.801 | 1.801 |
| ms | 321 | 1.791 | 1.790 |
| w | 407 | 1.754 | 1.754 |
| m | 1115 | 1.717 | 1.717 |
| s | 408 | 1.705 | 1.704 |
| vw | 414 | 1.657 | 1.657 |
| vw | 409 | 1.651 | 1.652 |
| vw | 3111 | 1.645 | 1.647 |
| s | 327 | 1.635 | 1.635 |
| m | 416 | 1.602 | 1.601 |

[a] Lattice is hexagonal $a_0 = 9.027(1)$, $c_0 = 27.843(6)$.

$K_8Ta_{14}Si_4O_{47}$ could be identified. The former predominated for values of $x < 0.5$, the latter for all other cases.

In order to see whether failure to incorporate P for Si was due to an instability associated with tunnel vacancies or to an instability of the linear $PSiO_7$ units, we attempted — unsuccessfully — to prepare $K_6(Ta_5Zr)(Si_3P)O_{26}$.

Similarly, we attempted—unsuccessfully—to prepare $K_6(Ta_5Zr)Si_4O_{25}F$. Moreover, the cation substitutions $K_5(Ta_5W)Si_4O_{26}$ and $K_3(Ta_3W_3)Si_4O_{26}$ proved equally unsuccessful, indicating a rather limited flexibility of the $(M_6Si_4O_{26})^{6-}$ framework.

In another direction, we investigated whether the framework would accommodate larger cations in the large-tunnel sites. We were unable to prepare either $Rb_6Ta_6Si_4O_{26}$ or $Rb_3Na_3Ta_6Si_4O_{26}$.

### *E. Small-Tunnel Interstitials*

There are three types of interstitial sites within the framework that are large enough to incorporate small cations such as $Li^+$ or $Mg^{2+}$; the 1(*a*) and 1(*b*) small-tunnel sites and 2(*c*). As a test of the $Li^+$ ion stability in any of these sites, we chose to prepare the system $Li_xK_6(Ta_{6-x}Zr_x)Si_4O_{26}$ in which charge compensation is accomplished within the framework. In this system, complete occupancy of the large-tunnel sites by $K^+$ ions forces the $Li^+$ ions into smaller sites. Single-phase products having the hexagonal framework were obtained for $x < 1.5$; extra lines appeared at greater compositions.

In the case of $Mg^{2+}$ ion interstitials in the system $Mg_xK_6(Ta_{6-2x}Zr_{2x})Si_4O_{26}$, significant contamination from other phases was already present at $x = 1$; even at $x = 0.5$, four very weak, unindexable lines were present.

Table VII summarizes the hexagonal lattice parameters for these cation-rich phases. Incorporation of the interstitial $Li^+$ or $Mg^{2+}$ ions, with concomitant substitution of $Zr^{4+}$ for $Ta^{5+}$ in the framework, causes an expansion of the lattice and of the axial ratio *c*/*a*. X-Ray emission spectra for $Mg_{0.5}K_6(Ta_5Zr)Si_4O_{26}$ gave a K : Ta ratio 1.09 : 1 (calc 1.20 : 1); a Ta : Si ratio 1.21 : 1 (calc 1.25 : 1); a Zr : Si ratio 0.24 : 1 (calc 0.25 : 1). Magnesium could be identified in the phase, but not accurately determined.

TABLE VII

CRYSTALLOGRAPHIC DATA FOR CATION-RICH PHASES[a]

| Phase | $a_0$ (Å) | $c_0$ (Å) | $V$ (Å$^3$) | *c*/*a* |
|---|---|---|---|---|
| $K_6Ta_6Si_4O_{26}$ | 9.066 | 7.873 | 560.4 | 0.8689 |
| $LiK_6Ta_5ZrSi_4O_{26}$ | 9.096(1) | 7.941(2) | 569.0 | 0.8730 |
| $Li_{1.5}K_6Ta_{4.5}Zr_{1.5}Si_4O_{26}$ | 9.114(1) | 7.948(1) | 571.8 | 0.8721 |
| $Li_2K_6Ta_4Zr_2Si_4O_{26}$[b] | 9.128(1) | 7.977(1) | 576.6 | 0.8739 |
| $Mg_{0.5}K_6Ta_5ZrSi_4O_{26}$ | 9.081(1) | 7.915(1) | 565.2 | 0.8716 |
| $MgK_6Ta_4Zr_2Si_4O_{26}$[b] | 9.104(2) | 7.951(3) | 570.7 | 0.8733 |

[a] All phases are hexagonal.
[b] Nominal composition.

The absence of single phases corresponding to the compositions $Li_xK_{6-x}Ta_6Si_4O_{26}$, $Li_{2+x}K_{6-x}(Ta_4Zr_2)Si_4O_{26}$, and $Li_{2x}Ba_{3-x}Ta_6Si_4O_{26}$ indicates that $Li^+$ ions are not stabilized in the pentagonal tunnels.

The phase $Li_xBa_3(Ta_{6-x}Zr_x)Si_4O_{26}$ could not be prepared pure, but a hexagonal phase was found with a cell volume larger than that of $Ba_3Ta_6Si_4O_{26}$.

Finally, in an attempt to reduce the Na/Ta ratio sufficiently to suppress formation of $NaTaO_3$, we fired mixtures corresponding to $Mg_xNa_{6-2x}Ta_6Si_4O_{26}$. For all *x*, mixed phases resulted in which $Na_2Ta_4O_{11}$ could be identified.

## Discussion

Bottleneck sizes in the $(Ta_6Si_4O_{26})^{6-}$ framework restrict high sodium ion mobility to the basal plane containing the 3(*g*) tunnel sites. It did not prove possible in this work to create more than three large-tunnel vacancies per formula unit, and the absence

of ionic motion strongly suggests that the 3(*g*) sites are always filled in nonstoichiometric derivatives. Choisnet *et al.* (*3*) attempted to determine the occupancies of the 3(*g*) and 3(*f*) sites by refining powder X-ray data for $K_{6-2x}Ba_xTa_6Si_4O_{26}$. The results were inconclusive due to the lack of quantity and precision of the data. We therefore attempted to study this problem by computing the ionic site potentials of the 3(*g*) and 3(*f*) sites in $K_6Ta_6Si_4O_{26}$ and $Ba_3Ta_6Si_4O_{26}$ using a computer program by Van Gool and Piken (*8*). In $K_6Ta_6Si_4O_{26}$ the potential at the 3(*g*) site, as calculated on a point-charge model, is over twice as favorable to cation occupancy as the 3(*f*) site. In $Ba_3Ta_6Si_4O_{26}$ the potential at the 3(*g*) site remains more favorable relative to that at the empty 3(*f*) sites. These findings were found to be independent of alterations in the charge distribution in the framework to simulate covalence; they imply, together with our experimental findings, that complete occupancy of the 3(*g*) sites is essential to the stability of this framework. It is for this reason that fast $Na^+$ ion motion is not observed.

Similar calculations for the $K_8Ta_{14}Si_4O_{47}$ structure imply the complete occupation of the 12(*k*) sites (which are known to be filled in $Ba_{6+x}Nb_{14}Si_4O_{47}$) with the extra $K^+$ ions occupying the 6(*g*) sites. Ionic motion is therefore not expected in this structure either.

A second question is the position of the extra $Li^+$ ions in $Li_xK_6(Ta_{6-x}Zr_x)Si_4O_{26}$ and related phases. To investigate this problem, we computed potentials at the 1(*a*), 1(*b*), and 2(*c*) sites for $K_6Ta_6Si_4O_{26}$. Surprisingly, we found that the 1(*a*) and 2(*c*) sites had comparable potentials and were much more favorable than the 1(*b*) positions. The origin of these results stems from the tilting of the octahedra along the *c* axis due to the necessity of matching the length of the $Si_2O_7$ pairs to that of pairs of octahedra. This causes an inward tilt of the oxygens around the 1(*a*) site together with a corresponding outward tilt of the tantalum atoms, thereby stabilizing the 1(*a*) cation position; whereas the opposite effect occurs around the 1(*b*) position. Thus for the 1(*a*) position there are three $O^{2-}$ ions at 2.19 Å and six at 2.55 Å, whereas for the 1(*b*) position there are three at 2.38 Å and six at 2.55 Å. The 2(*c*) site has six $O^{2-}$ ions at 2.22 Å, quite comparable to the 1(*a*) site. Calculations also show that the 1(*b*) site appears unfavorable in $Li_{1+x}K_6(Ta_{5-x}Zr_{1+x})Si_4O_{26}$; similar results are found for the magnesium analogs. It can be concluded that additional small cations enter either the 1(*a*) or the 2(*c*) sites.

Finally it is found that the chemical flexibility of the framework is limited by the range of possible alternative structures. In particular, large-tunnel vacancies, as created by substitution of $F^-$ for $O^{2-}$, P for Si, or W for Ta, result in the formation of the $K_8Ta_{14}Si_4O_{47}$ structure where the K:Ta ratio is lower. The large-tunnel sites appear to favor ions of the size of $K^+$, $Ba^{2+}$, $Sr^{2+}$; much smaller or larger ions, such as $Li^+$ and $Rb^+$, are more stable in other structures, although $Li^+$ may be stabilized in 1(*a*) or 2(*c*) positions. $Na^+$ ions are somewhat too small for the pentagonal tunnels so that other sodium tantalates, notably $NaTaO_3$, $Na_2Ta_4O_{11}$, and $Na_2Ta_8O_{21}$, become competitive at higher $Na^+$ ion concentrations. One particular competitive phase is the TKWB framework. In an attempt to identify the TKWB phase, we discovered a large solid-solution area in the $BaO–Na_2O–Ta_2O_5$ phase diagram where a $(TaO_3)^-$ framework has the TKWB structure and the interstitial tunnels are occupied by tantalum oxide groups as well as $Na^+$ and $Ba^{2+}$ ions.

**Acknowledgments**

We wish to thank Dr. A. Hamnett and Mr. A. R. Rae-Smith for assistance with the conductivity and X-ray emission experiments.

## References


1. J. SHANNON AND L. KATZ, *J. Solid State Chem.* **1,** 399 (1970).
2. J. SHANNON AND L. KATZ, *Acta Crystallogr. Sect. B* **26,** 105 (1970).
3. J. CHOISNET, N. NGUYEN, D. GROULT, AND B. RAVEAU, *Mater. Res. Bull.* **11,** 887 (1976).
4. D. M. EVANS AND L. KATZ, *J. Solid State Chem.* **8,** 150 (1973).
5. J. CHOISNET, N. NGUYEN, AND B. RAVEAU, *Mater. Res. Bull.* **12** 91 (1977).
6. J. CHOISNET, M. HERVIEU, D. GROULT, AND B. RAVEAU, *Mater. Res. Bull.* **12,** 621 (1977).
7. J. P. CHAMINADE, M. POUCHARD, AND P. HAGENMULLER, *Rev. Chim. Miner.* **9,** 381 (1972).
8. W. VAN GOOL AND A. G. PIKEN, *J. Mater. Sci.* **4,** 95 (1969).